A Construction for Computer Visualization of Certain Complex Curves

Andrew J. Hanson
Computer Science Department, Indiana University

Introduction

Computer graphics has proven to be a very attractive tool for investigating low-dimensional algebraic manifolds and gaining intuition about their properties [9]. In principle, a computer image of any manifold described by algebraic equations can be produced by numerically solving the equations [2] to generate a fixed tessellation, or by using equivalent ray-tracing techniques [5]. However, for high-performance *interactive* manipulation of a manifold, it is much simpler and more practical to have a parametric representation instead of an implicit equation that must be solved numerically; a significant additional feature of many parametric representations is that they embody symmetry information that can be used to further enhance the visualization process. Numerical solutions typically do not naturally emphasize natural structures of manifolds, are poorly behaved near singularities and self-intersections, and are more difficult to explore using other visualization tools such as submanifold selection, coordinate transformations, and deformations.

Therefore, in order to use mathematical visualization systems such as Mathematica [12], Maple [3], or Macsyma [11], or high-performance interactive systems such as Geomview [15] or MeshView [13], one would much prefer an explicit parametric representation of a manifold's geometry.

Driven by this motivation, we found an extremely useful construction for *parametric* models of large families of complex curves, that is, 2-manifolds representing the solutions of single equations in two complex variables or, equivalently, corresponding pairs of equations in four real variables. Our construction is ideally suited for interactive computer graphics systems; in addition, the resulting visualizations naturally exhibit subtle properties of the complex curves. This construction was first described in [7], where it was applied to the task of generating a computer animation [8] showing the properties of the homogeneous equations in CP^2 known as the "Fermat surfaces."

In Table 1, we list the Mathematica code [6] used to generate the illustrations shown in Figures 2, 6 and 7, as well as the analogous renderings in the Mathematica reference book [16]. Stewart Dickson has utilized this basic Mathematica model to realize the Fermat surfaces in the form of three-dimensional sculptures [14]; the physical model of the $n = 3$ Fermat surface shown in Figure 3 was created by Allan Lange at Hughes Aircraft in El Segundo, California, from Dickson's Mathematica specifications.

The Construction

Our construction is based upon a concept long familiar to the computer graphics community as the *superquadric* model of deformable curves and surfaces [1]. In two real dimensions, the superquadric curves

$$|x_1|^n + |x_2|^n = 1 \tag{1}$$

are interesting for shape modeling because, for continuous n, they interpolate between diamonds ($n = 1$), circles ($n = 2$), and squares ($n \to \infty$); superquadrics are essentially the level sets of L_n norms. Explicit parametric

representations of these curves are obtained by exploiting the identity

$$\cos^2\theta + \sin^2\theta = 1$$

and setting

$$\begin{aligned} x_1 &= \text{sign}(\cos\theta)|\cos\theta|^{2/n} \\ x_2 &= \text{sign}(\sin\theta)|\sin\theta|^{2/n} . \end{aligned}$$

We plot the resulting 2D curves in Figure 1 for various values of n. Similar techniques can be used in three or more dimensions to produce interpolations between (hyper)spheres and (hyper)cubes as well.

The homogeneous complexification of Eq. (1) for integer n leads to the Fermat surfaces, which are defined as solutions of the homogeneous equations in CP^2 of the form

$$(z_1)^n + (z_2)^n = (z_0)^n . \tag{2}$$

The hypothesis known as "Fermat's Last Theorem" reduces to the statement that the inhomogeneous form of this equation ($z_0 = 1$) has no real rational points for integer $n > 2$ and $\text{Re}(z_1) > 0$, $\text{Re}(z_2) > 0$.

The desired construction is derived by extending the superquadric method to the complex domain. We first recall that Eq. (2) can be represented locally in each of the three regular C^2 coordinate patches of CP^2: $z_0 \neq 0$, $z_1 \neq 0$, and $z_2 \neq 0$. For the purposes of computer graphics, we focus our attention on the case $z_0 \neq 0$, take local inhomogeneous coordinates z_i/z_0, and thus may locally set $z_0 = 1$ for all practical purposes. Equation (2) then becomes

$$(z_1)^n + (z_2)^n = 1 . \tag{3}$$

If we define the complex extensions of the sine and cosine,

$$\begin{aligned} u_1(\theta,\xi) &= \frac{1}{2}\left(\exp(\xi + i\theta) + \exp(-\xi - i\theta)\right) \\ u_2(\theta,\xi) &= \frac{1}{2i}\left(\exp(\xi + i\theta) - \exp(-\xi - i\theta)\right) , \end{aligned}$$

where

$$(u_1)^2 + (u_2)^2 = 1 , \tag{4}$$

we can verify that Eq. (3) is identically satisfied if we set

$$z_1(\theta,\xi,k_1) = s(k_1,n)u_1(\theta,\xi)^{2/n} \tag{5}$$

$$z_2(\theta,\xi,k_2) = s(k_2,n)u_2(\theta,\xi)^{2/n}, \tag{6}$$

where the phase factor

$$s(k,n) = \exp(2\pi ik/n) \tag{7}$$

is an nth root of unity for integers $0 \leq k \leq (n-1)$. We are not aware of any previous exploitation of this method for visualizing such surfaces.

Properties

The phase factors in z_1 and z_2 have n^2 combinations of values labeled by (k_1, k_2), and therefore Eq. (3) describes n^2 distinct quadrilateral patches in C^2 given by $(z_1(\theta,\xi,k_1),\ z_2(\theta,\xi,k_2))$ for $0 \leq \theta \leq \pi/2$ and $|\xi| \leq \xi_{\text{max}}$. Surfaces such as those shown in Figure 2 are found by piecing together the patches. Because the patches are related to one another by simple symmetry transformations, they have an *intrinsic* value for the viewer that numerical solutions would in general not be able to provide; in our own interactive MeshView system and in the Mathematica sample provided in Table 1, we exploit this fact by choosing color codes that are keyed to the pair (k_1, k_2), and thus automatically show the complex phase of any patch relative to the basis patch.

The characteristics of the surfaces can be understood in a number of ways. First, we note classical arguments determining the global topological invariants of these surfaces; then, we examine the way the patchwork quilt of n^2 segments fits together in the local coordinate system.

Euler Characteristic and Compactification Transform. The genus g of the surface follows from the Riemann-Hurwitz genus formula (see, e.g., [4]):

$$g = \frac{(n-1)(n-2)}{2} . \tag{8}$$

(The standard proof of this formula involves a topological picture quite different from the one we have presented.) The total Euler characteristic of the surface is then

$$\chi = 2 - 2g = 3n - n^2. \tag{9}$$

Thus we see that the $n = 2$ surface is a sphere ($g = 0$), $n = 3$ is a torus ($g = 1$), $n = 4$ is a 3-hole torus ($g = 3$), and so on.

Several transformations can be used to reexpress the surfaces so that they are finite in certain projections, and thus in principle allow one to deform them and examine the genus experimentally. One of the nicest of these is the transform

$$(z_1, z_2, z_0) \to \frac{(z_2 z_0, z_0 z_1, z_1 z_2)}{(|z_1|^2 + |z_2|^2 + |z_0|^2)^{1/2}} ,$$

which actually is an inversion mapping in inhomogeneous coordinates, swapping the singularities at $z_0 = 0$ for those at $z_1 = 0$ and $z_2 = 0$. Another is the (non-isomorphic) Riemann-sphere transform mapping C^2 to an S^4 with radius r; we define $\vec{\mathbf{x}} = (\mathrm{Re}(z_1), \mathrm{Im}(z_1), \mathrm{Re}(z_2), \mathrm{Im}(z_2))$ and take

$$\begin{aligned} \vec{\mathbf{u}} &= \frac{\vec{\mathbf{x}}}{(1 + |\vec{\mathbf{x}}|^2/(4r^2))} \\ u_0 &= 2r \frac{|\vec{\mathbf{x}}|^2/(4r^2)}{(1 + |\vec{\mathbf{x}}|^2/(4r^2))} \end{aligned}$$

to be the coordinates on an S^4 embedded in R^5 described by $|\vec{\mathbf{u}}|^2 + (u_0 - r)^2 = r^2$.

Patch Geometry. For a given integer n, as $|\xi| \to \infty$, the asymptotic surface boundaries consist of n circles approaching different points on the complex line $z_0 = 0$ at projective infinity. When $\xi = 0$, we see that at $\theta = 0$ we have $z_1 = s(k_1, n)$, $z_2 = 0$, while at $\theta = \pi/2$, $z_1 = 0$, $z_2 = s(k_2, n)$. Figure 4 shows the appearance of a single patch for fixed (k_1, k_2). The $2n$ surface points with $z_1 = 0$ or $z_2 = 0$ are the fixed points of the cyclic group of complex phase transformations $z_1' = \exp(i\phi_1) z_1$, or $z_2' = \exp(i\phi_2) z_2$. n additional such points occur where the asymptotic circles intersect the complex line $z_0 = 0$ at projective infinity, giving the expected total of $3n$ fixed points of the cyclic group of phase transformations.

In general, n patches meet in a highly hyperbolic pie-chart arrangement at each end of the $\xi = 0$ axis. In Figure 5, we examine the $n = 3$ Fermat surface (which is the only flat example) and show how the 9 patches labeled by (k_1, k_2) are related to one another; the small shaded circles labeled by $p[q]$ correspond to fixed points of the complex phase transformations, where one variable vanishes, $z_p = 0$, and the other is of the form $z = \exp(2\pi i q/n) = \exp(2\pi i q/3)$; the large shaded hexagons are the analogous 3 points where the boundary circles intersect the projective line at infinity, where $z_0 = 0$. The toroidal topology can be seen directly be joining the centers of the four dark-shaded hexagons.

Extensions to Related Equations

Once the generalization of the superquadric construction to produce solutions of the complex Fermat equation was understood, we realized that several other classes of polynomial equations could be parameterized using analogous techniques.

Torus-Knot-Like Boundaries. When we take two different powers of the complex variables,

$$(z_1)^{n_1} + (z_2)^{n_2} = 1 , \tag{10}$$

we can parameterize the (now inhomogeneous) surface using

$$z_1 = s(k_1, n_1)(u_1)^{2/n_1} \tag{11}$$

$$z_2 = s(k_2, n_2)(u_2)^{2/n_2}, \tag{12}$$

for $0 \le \theta \le \pi/2$ and $|\xi| \le \xi_{\max}$. These functions give $n_1 \times n_2$ different phase-related patches that cover the finite portion of the surface.

This is a surface with boundary that at large distances is asymptotic to the solutions of the torus knot variety,

$$(z_1)^{n_1} + (z_2)^{n_2} = 0 \tag{13}$$

(i.e., imagine scaling by a large denominator as $\xi_{\max}$ becomes large), except with the boundary given by the intersection with

$$|z_1|^{n_1} + |z_2|^{n_2} = |u_1|^2 + |u_2|^2 = \cosh 2\xi_{\max} \tag{14}$$

instead of the traditional unit 3-sphere. Some examples are shown in Figure 6.

Product Polynomials. Another extension to product polynomials is straightforward. Consider the homogeneous equation

$$(z_1)^{n_1} (z_2)^{n_2} = (z_0)^{n_1 + n_2} \tag{15}$$

and its inhomogeneous form

$$(z_1)^{n_1}\,(z_2)^{n_2} = 1\ . \tag{16}$$

If we take

$$\begin{aligned} z_1 &= (u_1 + iu_2)^{1/n_1} \\ &= s(k_1, n_1)\exp[(i\theta + \xi)/n_1] \qquad (17) \\ z_2 &= (u_1 - iu_2)^{1/n_2} \\ &= s(-k_2, n_2)\exp[-(i\theta + \xi)/n_2], \qquad (18) \end{aligned}$$

then we get a single-valued parameterization that covers the entire surface using $n_1 \times n_2$ patches (note that $-k_2$ seems to be a more natural convention). We choose the variable ranges $0 \le \theta \le 2\pi$ and $|\xi| \le \xi_{\max}$ to get the required patch ranges. This is slightly peculiar because the basic patch here is essentially four times the size of the basic patch for the Fermat surfaces; these surfaces may be easier to see if different colors or markings are used for subsets of the basic $0 \le \theta \le 2\pi$ range.

And So On... Superquadric models have been applied to all sorts of variations of the equation of the circle $x^2 + y^2 = 1$ that we have used as the basis for the 2-manifolds shown here. For example, one can easily choose polar coordinates on a higher-dimensional sphere such as $x^2 + y^2 + z^2 = 1$ with

$$\begin{aligned} x &= \cos\theta \sin\phi \\ y &= \sin\theta \sin\phi \\ z &= \cos\phi \end{aligned}$$

and make a complex substitution $\cos\theta \to u_1(\theta, \xi)$, $\sin\theta \to u_2(\theta, \xi)$, $\cos\phi \to v_1(\phi, \chi)$, $\sin\phi \to v_2(\phi, \chi)$, where $u_1 \pm iu_2 = \exp(\pm i\theta \pm \xi)$ and $v_1 \pm iv_2 = \exp(\pm i\phi \pm \chi)$, to get a basis for a local C^3 coordinate system, $(x \to z_1, y \to z_2, z \to z_3)$, in CP^3; applying techniques analogous to those we used for surfaces (including using differing exponents for u_i and v_i) yields various families of 4-manifolds. There are obviously an enormous number of variants; unfortunately, our ability to do meaningful graphics degrades rapidly with increasing manifold dimension!

Remarks

Complex algebraic equations are interesting objects for study using computer graphics techniques. The Fermat surfaces in fact correspond topologically to Riemann surfaces for n-th roots in the complex plane with appropriate branch cuts; graphically exploring the explicit deformation between the algebraic form and the traditional branching structure of the corresponding Riemann surfaces is another fascinating exercise that we have no space to elaborate on here (see, e.g., [10]). The family of parametric constructions we have presented easily allows the interactive examination of the surfaces and their global topology, as well as exhibiting the complex phase relations and fixed points on the surfaces through the use of phase-related color codes on the patches.

Acknowledgements

This work was supported in part by NSF grant IRI-91-06389. I am grateful to Jon Barwise for originally encouraging me to write up this material for *Computers and Mathematics*. Special thanks are due to John Ewing and Chuck Livingston for their patience in setting me on the right track during the early stages of this work. My students Pheng Heng and Hui Ma have provided indispensable computer graphics tools for interactive renderings of these surfaces. The remarkable sculpture shown in Figure 3 was provided courtesy of Hughes Aircraft Company through the diligent efforts of Allan Lange and Stewart Dickson. Some of this material was originally presented at the Colloquium on Computer Graphics in Pure Mathematics, Iowa City, Iowa, May 17–19, 1990; I gratefully acknowledge Dennis Roseman's hospitality. The treatment of inhomogeneous surfaces was inspired by conversations with David Mumford; Lee Rudolph encouraged me to add product surfaces.

References

[1] A.H.Barr. Superquadrics and angle-preserving transformations. *IEEE Computer Graphics and Applications*, 1:11–23, 1981.

[2] J. Bloomenthal. Polygonalization of implicit surfaces. *Computer Aided Geometric Design*, 5:341–355, 1988.

[3] B.W. Char, K.O. Geddes, G.H. Gonnet, B.L. Leong, M.B. Monagan, and S.M. Watt. *Maple V Language Reference Manual*. Springer-Verlag, New York, 1991.

[4] P. Griffiths and J. Harris. *Principles of Algebraic Geometry*. Wiley, 1978.

[5] P. Hanrahan. Ray tracing algebraic surfaces. In *Computer Graphics (SIGGRAPH '83 Proceedings)*, volume 23, pages 83–90, July 1983.

[6] A. J. Hanson. Solutions of Fermat's equation, March 1994. Mathematica notebook 0206-288, available from the MathSource server at `mathsource@wri.com`.

[7] A. J. Hanson, P. A. Heng, and B. C. Kaplan. Techniques for visualizing Fermat's last theorem: A case study. In *Proceedings of Visualization 90*, pages 97–106, San Francisco, October 1990. IEEE Computer Society Press.

[8] A. J. Hanson, P. A. Heng, and B. C. Kaplan. Visualizing Fermat's last theorem. *SIGGRAPH Video Review*, 61(4), 1990. 3:37 minute video animation.

[9] A.J. Hanson, T. Munzner, and G.K. Francis. Interactive methods for visualizable geometry. *IEEE Computer*, 27(7):73–83, July 1994.

[10] P. Heng. *Interactive Visualization Tools for Topological Exploration*. PhD thesis, Indiana University, 1992.

[11] Macsyma Inc. *Macsyma*. Macsyma, Inc., Cambridge, MA, 1993.

[12] Wolfram Research Inc. *Mathematica*. Wolfram Research, Inc., Champaign, IL, version 2.1 edition, 1992.

[13] H. Ma and A.J. Hanson. Meshview. A portable 4D geometry viewer written in OpenGL/Motif, available by anonymous ftp from geom.umn.edu, The Geometry Center, Minneapolis MN.

[14] I. Peterson. Plastic math: Growing plastic models of mathematical formulas. *Science News*, 140(5):72–73, August 1991. Description of the work of Stewart Dickson on creating mathematical sculptures; see also vol. 140, no. 17, Oct. 26, 1991, p. 259.

[15] M. Phillips, S. Levy, and T. Munzner. Geomview: An interactive geometry viewer. *Notices of the Amer. Math. Society*, 40(8):985–988, October 1993. In the "Computers and Mathematics" column. Available by anonymous ftp from geom.umn.edu, The Geometry Center, Minneapolis MN.

[16] S. Wolfram. *Mathematica, A System for Doing Mathematics by Computer*. Addison-Wesley, Redwood City, CA, second edition, 1991. See pages 38–39.

The parametric functions:

```
cCos[theta_,xi_] := .5(E^(xi + I theta) + E^(- xi - I theta))
cSin[theta_,xi_] := (-.5 I)(E^(xi + I theta) - E^(- xi - I theta))
z1[theta_,xi_,n_,k_] := E^(k*2*Pi*I/n)*cCos[theta,xi]^(2.0/n)
z2[theta_,xi_,n_,k_] := E^(k*2*Pi*I/n)*cSin[theta,xi]^(2.0/n)
pz1[theta_,xi_,n_,k_] := E^(( xi + I theta)/n)*E^( k*2*Pi*I/n)
pz2[theta_,xi_,n_,k_] := E^((- xi - I theta)/n)*E^(-k*2*Pi*I/n)
```

Polygon Construction: See `Mathematica:Packages:Graphics:ParametricPlot3D.m`.

```
MakePolygons[vl_List] :=
    Block[{l = vl, l1 = Map[RotateLeft, vl], mesh},
 mesh = {l, l1, RotateLeft[l1], RotateLeft[l]};
 mesh = Map[Drop[#, -1]&, mesh, {1}];
 mesh = Map[Drop[#, -1]&, mesh, {2}];
 Polygon /@ Transpose[ Map[Flatten[#, 1]&, mesh] ]]
```

Construct and display Fermat Surface:

```
n1 = 3; n2 = 3;  xiSteps=17; xiMax = 1;  thetaSteps=17; angle = Pi/4;
   cosA = Cos[angle];  sinA = Sin[angle];
Do[ Do[ patch33[k1+1,k2+1] =
          MakePolygons[Table[
             Block[{z1Val = N[z1[theta,xi,n1,k1]],
                    z2Val = N[z2[theta,xi,n2,k2]]},
        {Re[z1Val], Re[z2Val], cosA*Im[z1Val] + sinA*Im[z2Val]}],
               {xi,-xiMax,xiMax,(2*xiMax)/(xiSteps - 1)},
               {theta,0,Pi/2,(Pi/2)/(thetaSteps - 1)}]],
         {k1,0,n1-1}],
    {k2,0,n2-1}];
```

Power surface: Replace `zi` $\rightarrow$ `pzi` and `Pi/2` $\rightarrow$ `2 Pi`.

Place actual drawing on screen, color code the patches.

```
bs0 = 0.8; bs1 = 0.2; lt = 0.9;
surface33=
  Show[
   Graphics3D[
     Table[[Block[{bs = If[And[k1==0 , k2==0],bs0,bs1]},
           {RGBColor[bs+lt*k1/(n1-1),bs+lt*k2/(n2-1),bs],
            patch33[k1+1,k2+1]}]
            {k1, 0, n1-1}, {k2, 0, n2-1}],
     Lighting->False, Axes->None, Boxed -> False, BoxRatios->{1,1,1},
     ViewPoint->{2.9, 1.0, 1.4} ]]
```

Table 1: Mathematica expressions for the explicit parameterization and plotting of the solutions to Eqs. (3), (10), and (15). Massive amounts of memory are required to render the surfaces with nontrivial parameter ranges `xiSteps` and `thetaSteps`. `xiSteps` must be *odd* to guarantee that the surface will pass through the fixed points at $(\theta, \xi) = (0, 0)$ and $(\theta, \xi) = (\pi/2, 0)$ and avoid anomalies in the surface representation.

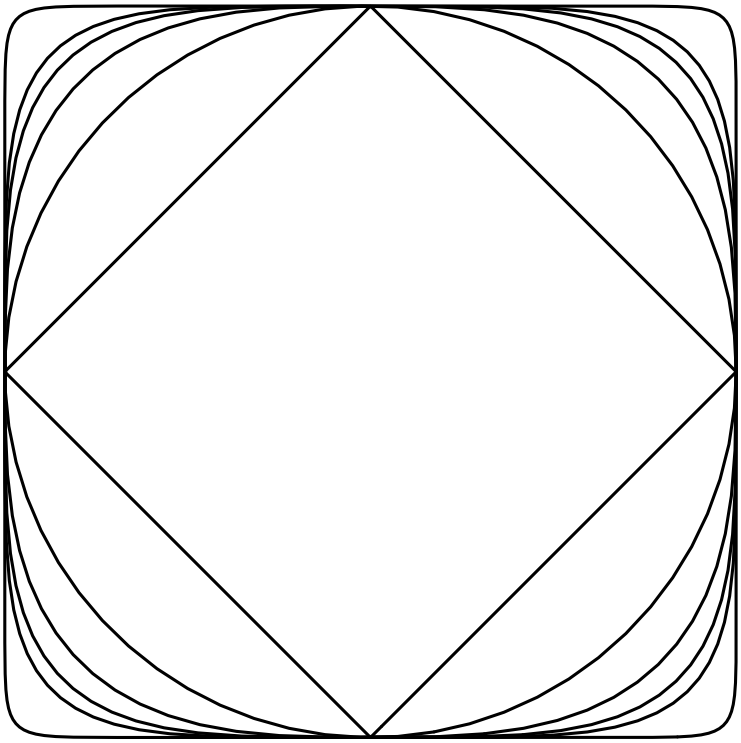

Figure 1: Real superquadric 2D shapes for several values of n.

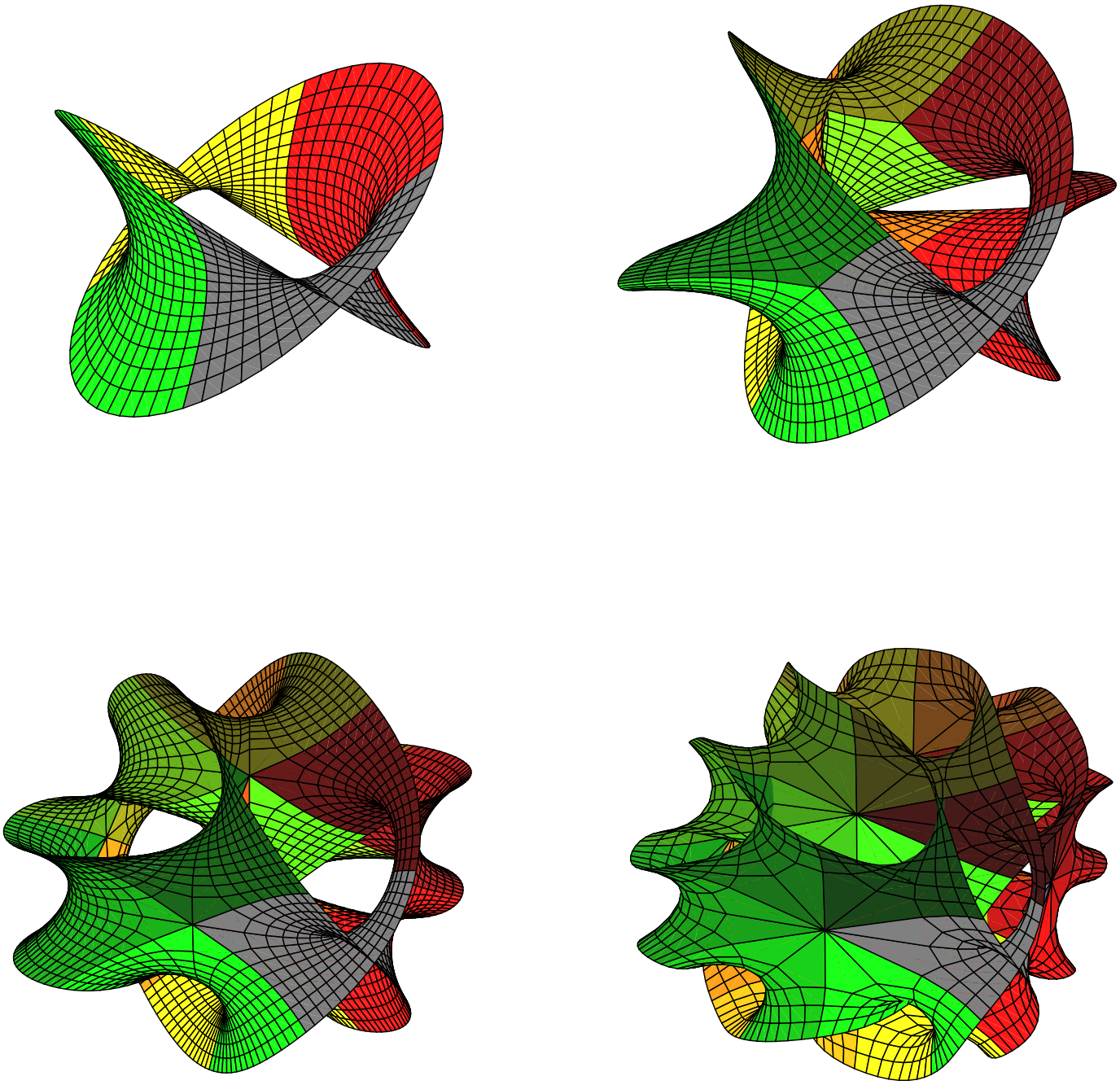

Figure 2: (a) One view of the surface obtained by projecting Eq. (3) for $n = 2$ from 4D to 3D. (b) The $n = 3$ surface. (c) The $n = 4$ surface. (d) The $n = 6$ surface.

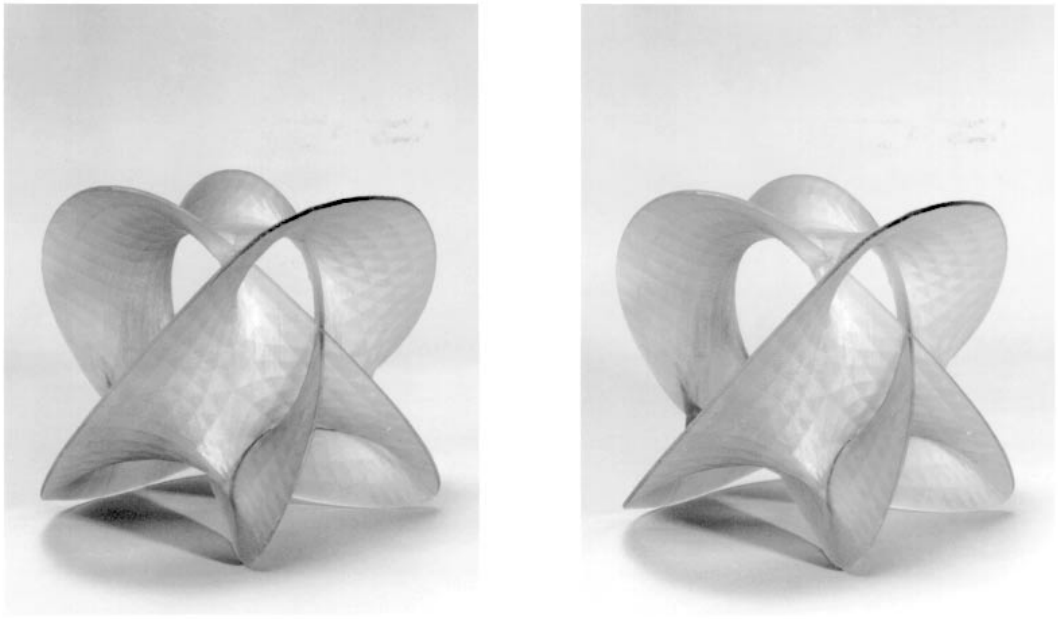

Figure 3: A mathematically accurate 3D plastic model of the surface Eq. (3) for $n = 3$ projected from 4D to 3D. This stereo pair may be viewed cross-eyed to produce a 3D image.

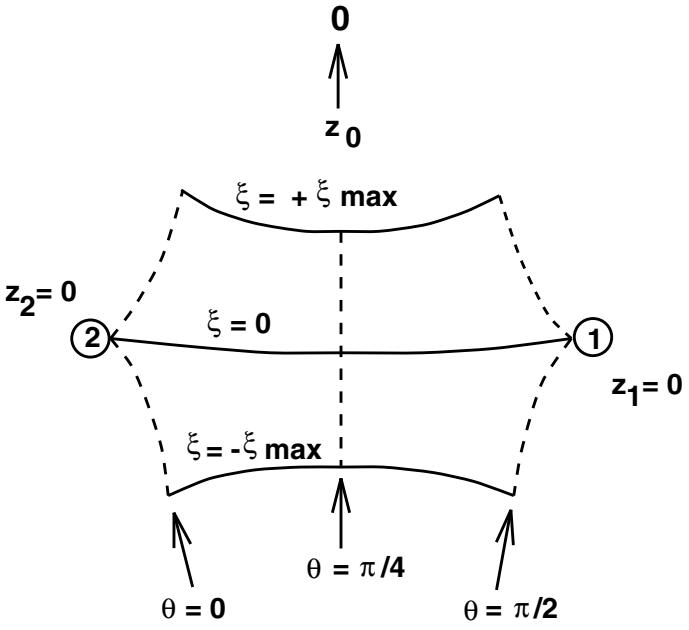

Figure 4: The shape of a single patch out of the n^2 parametric patches making up the Fermat surface of degree n.

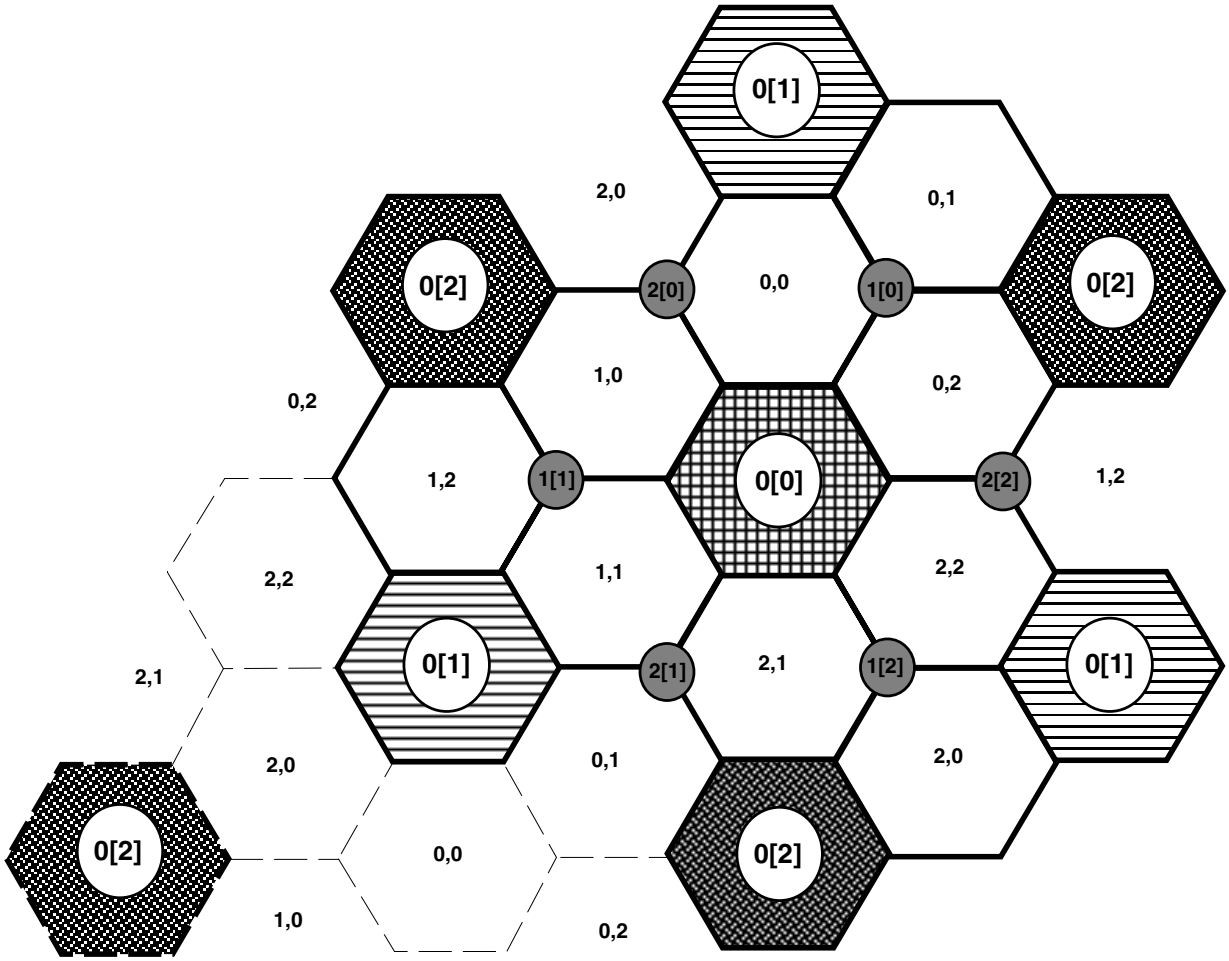

Figure 5: The relationships and relative phases of the 9 patches of the $n = 3$ (genus one) toroidal Fermat surface labeled by (k_1, k_2). The six small circles labeled by $p[q]$ are points where $z_p = 0$ and the other variable takes the value $z = \exp(2\pi iq/3)$; the shaded hexagons correspond to the three analogous points at projective infinity. The toroidal structure of this surface is obvious if one joins the centers of the four copies of the dark-shaded hexagon labeled $0[2]$.

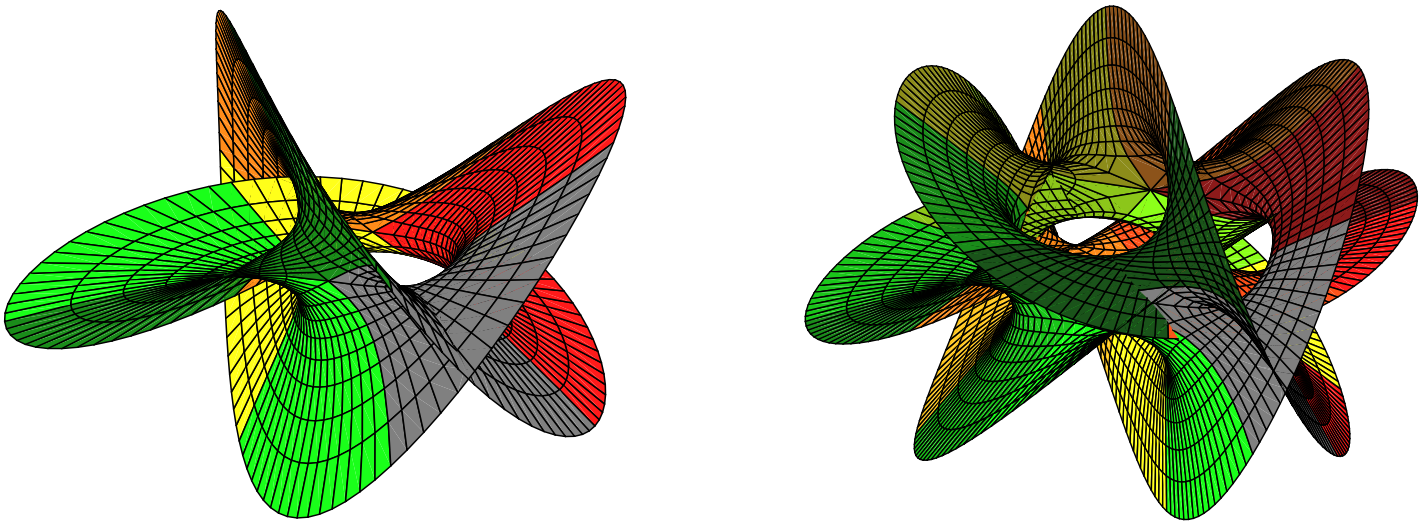

Figure 6: Generalizations of the construction to include torus-knot-like boundaries of the finite complex surfaces. The $(2, 3)$ and the $(3, 5)$ surfaces described by Eq. (10) are shown here.

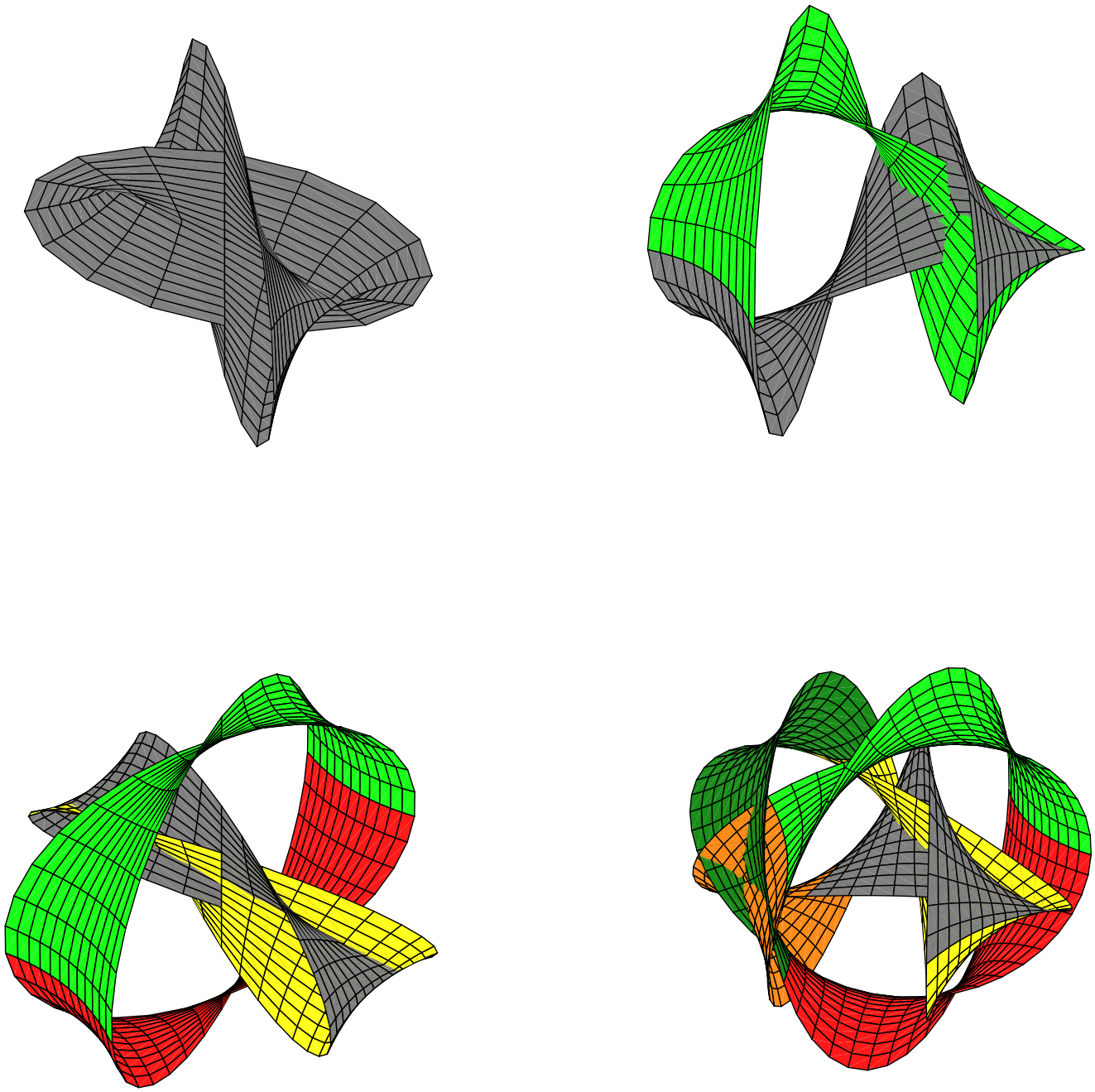

Figure 7: Products of polynomials generating two-manifolds in C^2. The surfaces with powers $(1,1)$, $(1,2)$, $(2,2)$, and $(2,3)$ given by Eq. (15) are shown.